Alpha particle physics in a tokamak burning plasma experiment

W.W. Heidbrink, University of California, Irvine, CA 92697
email: wwheidbr@uci.edu

ABSTRACT.

Much is known about the behavior of energetic ions in tokamak devices but much remains to be understood. Single-particle effects are well understood and provide a firm basis for extrapolation to a burning plasma. In contrast, collective effects involving fast ions are more poorly understood and extrapolations are unreliable. Collective modes of concern include toroidicity-induced and ellipticity-induced Alfvén eigenmodes (TAE and EAE), kinetic ballooning modes, and internal kink modes. In addition to these magneto-hydrodynamic (MHD) normal modes, there are also energetic particle modes characterized by strong dependence on the fast-ion distribution function. Although many issues are important areas of study in current experiments, five issues distinguish burning plasma experiments. First, the energetic alphas are not the dominant source of free energy for the instabilities unless the fusion power exceeds the heating power by a factor of ten. Second, the damping of the instabilities depends sensitively on mode coupling to other heavily-damped waves. The magnitude of this coupling is expected to depend on the normalized thermal gyroradius, which is much smaller in a reactor. Third, in a reactor, both the radial extent of the instabilities and the fast-ion orbit contract relative to current experiments, so the fast-ion transport will change. Fourth, when instability occurs, a larger number of modes are unstable, so the mechanism of nonlinear saturation could shift from fast-ion transport to mode coupling. Fifth, because of the extreme sensitivity of energetic particle modes to the distribution function, an isotropic alpha particle distribution

function differs from anisotropic fast-ion populations.

I. INTRODUCTION

A typical tokamak plasma contains thermal electrons, thermal ions, and a population of suprathermal fast ions produced by fusion reactions, neutral-beam heating, or radio-frequency heating in the ion cyclotron range of frequencies (ICRF). The results from thirty years of study are summarized in review papers by Heidbrink and Sadler [1] and the International Thermonuclear Experimental Reactor (ITER) Energetic Particle Expert Group [2]. Other noteworthy review papers include a summary of alpha-particle experiments on the Tokamak Fusion Test Reactor (TFTR) by Zweben *et al.* [3] and a summary of experimental observations of the toroidicity-induced Alfvén eigenmode (TAE) by Wong [4]. The goal of this paper is to use this extensive knowledge base to identify key alpha-particle physics issues that require a "burning" plasma experiment for clarification. By assumption, the alpha particles are produced in a deuterium-tritium (DT) tokamak plasma with a ratio of fusion power to heating power (Q) that exceeds ten. After a status report on our understanding of alpha-particle physics based on current experiments in Sec. 2, the paper discusses five issues involving fast-ion driven instabilities that require a reactor-scale experiment for definitive testing.

II. FAST-ION PHYSICS IN CURRENT DEVICES

On the eve of high-power DT experiments in TFTR and the Joint European Torus (JET), Heidbrink and Sadler reviewed the previous experimental studies of fast ions in tokamaks [1]. Their paper contains a number of summary figures on topics such as the effective diffusion of fast ions. In every case where a definitive prediction based on prior experiments was made, the prediction was confirmed by the subsequent DT experiments. Indeed, in his review of the TFTR DT experiments, Strachan overlaid the new alpha-particle data on the previous summary figures [5]. Figure 1 shows one ex-

ample. Because these predictions were already vindicated in the first DT experiments, they also apply with a high degree of confidence to the next generation of burning plasma experiments.

The individual behavior of dilute populations of alphas ("test particles") is well understood [1, 2]. The alpha production rate, initial energy, and birth profile are governed by the DT fusion reaction. Once they are born, the alphas decelerate due to Coulomb collisions at the rate predicted by standard small-angle scattering theory (Fig. 1). The initial orbit is given by drift-orbit theory. The toroidal field ripple associated with a discrete number of field coils causes additional losses that are in reasonable agreement with the calculated values. Background magnetohydrodynamic (MHD) activity such as the sawtooth crash or large tearing modes also cause fast-ion transport that has been successfully modeled. Turbulent transport associated with short-wavelength fluctuations is one-to-two orders of magnitude smaller than thermal transport, presumably because the large *fast-ion* gyroradius decorrelates the fast ions from fluctuations with a scale length comparable to the *thermal-ion* gyroradius. These findings indicate that, in a burning plasma experiment, the necessary conditions exist for producing a sufficiently intense alpha-particle population to study collective modes that are destabilized by the alpha particles.

In contrast, despite intensive study, fast-ion driven instabilities are more poorly understood. One difficulty is the large number of instabilities that have been observed (Fig. 2). One family of instabilities are the Alfvén eigenmodes (AE). Departures from cylindrical symmetry introduce gaps in the shear Alfvén continuum of ideal MHD [6]. Unstable eigenmodes exist in the gap caused by toroidicity, ellipticity, and triangularity [7]. There is also a core-localized version of the TAE [8] and a normal mode caused by finite Lar-

mor radius effects, the KTAE [9]. Other instabilities at higher frequencies include ion-cyclotron emission (ICE) [1] and compressional Alfvén eigenmodes [10]. At low frequencies, there is the fishbone instability, which is an internal kink with a toroidal mode number of $n = 1$ [1], and kinetic ballooning modes (KBM) [11]. All of these modes exist as stable waves even in the absence of a plasma population. Indeed, many of these modes have been studied with an internal antenna in ohmically heated plasmas [12]. However, there is another class of fast-ion driven instabilities, the energetic particle modes [13] (Table I). In contrast to the MHD modes, these only exist in plasmas with a significant energetic ion population. The mode structure resembles the eigenfunction of the related MHD mode, but the energetic particle mode constitutes a separate wave branch with a distinctive dispersion relation. Both the frequency and growth rate depend sensitively on the fast-ion distribution function, with the frequency usually corresponding to a characteristic frequency of the fast-ion motion. The most familiar example is the fishbone instability. The first observation [14] was the energetic particle mode branch with a frequency close to the precession frequency of the injected beam ions. Later, fishbones with a frequency close to the frequency expected for the MHD wave were observed (Table IV of Ref. [1]). Unstable energetic particle mode branches have been observed for the KBM and the TAE [15, 16]. These energetic particle modes are also called r-KBM and r-TAE [17]. (The "r" stands for "resonant.")

In addition to the large number of instabilities, an additional complication is that a large number of properties are required to specify completely the wave behavior. Basic characteristics include the wave frequency and structure (in all three dimensions) and the wave polarization (which has an important effect on possible resonant transport). Linear stability depends on

the competition between the damping rate and the drive term. The damping rate is associated with collisionless (Landau) and collisional interaction with the thermal plasma, as well as mode coupling to heavily damped waves. The fast-ion drive term is associated with free energy extracted from the fast-ion population. If the mode is linearly unstable, the subsequent transport of fast ions is important. Finally, knowledge of all of these factors is required for a thorough understanding of nonlinear saturation of the instability.

Given the number of instabilities and the complexity of the problem, it is not surprising that relatively few theoretical predictions have been thoroughly benchmarked by experiment. Table II provides an admittedly subjective assessment of the status of the benchmarking for three important instabilities: the fishbone (EPM branch), the TAE, and the r-TAE. Although much has been learned, it is evident that great progress in understanding is still possible. Concerted effort and diagnostic innovations in existing devices are as important to the progress of the field as a burning plasma experiment.

III. UNIQUE ISSUES IN A BURNING PLASMA EXPERIMENT

A. Alphas dominate when $Q \gtrsim 10$

By definition, fast-ion driven instabilities derive their free energy from the fast-ion distribution function. In general, gradients in both velocity space and configuration space are important. Consider the simplified expression for the alpha-particle drive of the TAE mode derived by Fu and VanDam [18], which is proportional to

β_α	$(\omega_{*\alpha}/\omega$	$-$	$\frac{1}{2})$	$F(v_\alpha/v_A)$
alpha	spatial		velocity	resonant
beta	gradient		space	fraction

This expression illustrates several generic features of the fast-particle drive.

- The drive is proportional to the number of fast ions in the plasma.

- The $\omega_{*\alpha}$ term represents free energy associated with the spatial gradient that is tapped by the wave. ($\omega_{*\alpha}$ is the alpha particle diamagnetic drift.) For TAEs driven by circulating fast ions, this occurs because the orbital shift of passing particles transfers energy from an interior flux surface to a larger radius flux surface [19].

- Depending on the distribution function, the velocity space term can be stabilizing or destabilizing. For the Maxwellian isotropic distribution function considered by Fu and VanDam, the wave Landau damps on the fast ions, so the contribution is stabilizing. However, for anisotropic or non-monotonic distribution functions, the velocity space term can help drive the instability.

- The strength of the drive term depends on the fraction of the distribution function that satisfies a resonance condition between the wave phase velocity and the particle velocity. This is represented by the function F for the particular distribution function considered by Fu and VanDam.

The alpha particle distribution function in a reactor is a nearly isotropic, slowing-down distribution. In contrast, the distribution function produced by neutral-beam heating is an anisotropic, slowing-down distribution function. The distribution function produced by ICRF heating is an anisotropic, Boltzmann distribution. Clearly, the fast-ion drive term associated with alpha-particle heating differs considerably from the fast-ion drive (or damping) term associated with auxiliary heating.

A high fusion power multiplication factor Q is necessary to access a regime where the alpha-particle distribution predominates. In steady state, $Q \simeq$ (fusion power)/(heating power). By the nature of the DT fusion reaction,

alphas only obtain 20% of the released energy (with 80% carried by the 14-MeV neutron). In most contemporary tokamak experiments, fast ions constitute nearly 100% of the heating power. Assume that all of the fast-ion species have similar spatial profiles and are well confined. Then, after combining these factors, we find that the ratio of the alpha-particle pressure to the fast-ion pressure from auxiliary heating sources is

$$p_\alpha / p_{heat} \sim \frac{Q}{5}. \tag{1}$$

Equation 1 implies that, roughly speaking, alpha particle drive effects become twice as important as auxiliary heating effects only for $Q \gtrsim 10$. In contrast, for $Q \sim 1$ as in the TFTR and JET DT experiments, the fast ions from auxiliary heating play a dominant role. This is nicely illustrated by a TFTR experiment that successfully observed alpha-particle driven TAEs [11]. During the main heating pulse, beam ions constitute a significant fraction of the total plasma beta, which is an order of magnitude larger than the alpha-particle beta (Fig. 3). In order to isolate the alpha-particle effects, the neutral beam injectors are turned off. In the "after-glow" phase of the discharge, the beam ions decelerate faster than the alpha particles, so a condition is transiently achieved where the alpha particle population is larger than the beam-ion population. During this phase, the alpha-particle instability drive overcomes ion Landau damping on the beam-ion population and TAEs with toroidal mode numbers n of 2-5 are observed. The limit implied by Eq. 1 is a severe restriction in contemporary devices. All of the TFTR experiments on collective alpha-particle effects required clever techniques to isolate the relatively small alpha-particle contributions [3].

B. Mode damping may change in reactor-scale experiments

The second important difference between current experiments and a burning plasma experiment concerns the damping of fast-ion instabilities by the

background plasma. A DT plasma is not required to study this effect but a reactor-scale experiment is.

Consider the linear damping of the TAE. The wave can damp through collisional or collisionless (Landau) damping on the electrons, through damping on thermal ions, or through mode coupling to other damped waves. In current experiments, calculations indicate that direct wave damping on thermal particles is too small to account for the observed damping rates [4]. Coupling to other waves such as the kinetic Alfvén wave is thought to dominate the damping rate in most cases. Evidence in support of this view include the observation of kinetic Alfvén waves during TAE experiments on TFTR [20] and the agreement between JET damping measurements and calculations of wave damping by a code that includes coupling to other waves as a primary damping mechanism [21]. Theoretically, mode coupling rates depend sensitively on the proximity of the dispersion relations of the two waves in $k - \omega$ space. Experimentally, the measured damping rates often vary an order of magnitude for slight changes in plasma parameters [22], in qualitative support of a sensitive dependence.

Mode coupling of the TAE to kinetic Alfvén waves was called radiative damping by Mett and Mahajan [23]. In their theory, the damping rate depends on the gyroradius $\rho_s = \sqrt{T_e m_i}/ZeB$ (because kinetic Alfvén waves are associated with finite thermal Larmor radius effects). Their prediction that the damping should depend on the gyroradius normalized to the plasma minor radius $(\rho_s^*)^{2/3}$ is not in quantitative agreement with experimental measurements [24] but the general expectation that the normalized gyroradius is an important parameter in mode coupling calculations is widely accepted theoretically.

In a reactor, the normalized gyroradius will decrease. Other damping

mechanisms have other scalings. For example, ion Landau damping depends on the ratio of the thermal ion velocity to the Alfvén speed, $v_i/v_A \propto \sqrt{n_e T_i}/B$, with no explicit dependence on machine size. Thus, in reactor-scale plasmas, the importance of mode coupling relative to other damping mechanisms will shift.

C. Changes in fast-ion transport

Unstable fast-ion driven instabilities cause transport of the fast ions. Whereas resonant convective transport to the walls can occur in contemporary experiments, redistribution is likely in a burning plasma experiment.

To illustrate this effect, consider the best documented case of fast-ion transport caused by an instability, the precessional-drift fishbone in the Poloidal Divertor Experiment (PDX). The beam-ion losses were explained by the "mode-particle pumping" theory proposed by White et al. [25]. This theory begins with an MHD calculation of the eigenfunction of the $n = 1$ internal kink mode (Fig. 4). The different poloidal harmonics extend throughout the plasma volume. In the presence of this wave, both analytical theory and numerical calculations show that a beam ion on an ordinary banana orbit can remain in phase with the wave across the entire plasma. A convective $\mathbf{E} \times \mathbf{B}$ drift to large major radius occurs and the beam ion is lost to the wall after only a few banana orbits. This theory was successfully compared with measurements from an impressive suite of fast-ion diagnostics including neutron detectors, several charge exchange sightlines, a fast-response diamagnetic loop, a lost-ion detector, and a ^{3}He burnup diagnostic [1].

Measurements in the DIII-D tokamak indicate that large convective losses of beam ions can occur during TAE activity too [26]. However, the relevance of these results to larger devices is questionable for two reasons. First, as discussed in the next section, the most unstable toroidal mode number for

the TAE is likely to shift to higher values in a burning plasma experiment. Roughly speaking, the radial extent of a TAE is inversely proportional to n, so the eigenfunction is unlikely to extend completely across the plasma, as it did for the PDX fishbone experiments (Fig. 4). Second, the size of the fast-ion orbit relative to the minor radius is smaller in a burning-plasma experiment, which also tends to reduce the magnitude of the transport. As shown in Table III, both the expected orbit size ρ/a and the radial mode extent are a factor of ~ 5 smaller in a burning-plasma experiment. Consequently, redistribution of the fast-ion population rather than losses may occur.

D. Nonlinear saturation due to a "sea" of unstable modes

In current experiments, the nonlinear saturation of fast-ion driven instabilities is often controlled by the loss of fast ions. For example, in both the PDX fishbone experiments and the DIII-D TAE experiments, a repetitive pattern of instability bursts and beam-ion losses were observed. This burst cycle was successfully explained by a semi-empirical "predator-prey" model, where the growth of the beam-ion population is halted by the "death" of the fast ions when the mode expels them to the wall [27]. Because of changes in fast-ion transport and changes in the mode spectrum, this mechanism is unlikely to govern nonlinear saturation in a burning plasma experiment.

Consider the TAE. Theoretically, the alpha particle drive increases with increasing mode number until the fast-ion gyroradius exceeds the width of the mode (Fig. 5a). The most unstable toroidal mode occurs near the maximum of the growth rate for values of $k_\theta \rho_\alpha \sim 1$. ($k_\theta$ is the poloidal wavenumber of the TAE.) In the experiments, the toroidal mode number n is reliably measured. Reexpressing this prediction in terms of n, the most unstable

toroidal mode number is approximately

$$n \simeq aB_T/(qZ_f\sqrt{8E_f m_f}). \tag{2}$$

Comparison with observations from several tokamaks shows that this expression is in rough agreement with experimental observations (Fig. 5b). The general trends that n increases with toroidal field and decreases with safety factor are also observed for comparisons on individual tokamaks. Hence, in a burning plasma experiment where aB_T is large, the most unstable toroidal mode number is expected to shift to larger mode numbers.

This has important implications for the number of modes that are unstable. Figure 6 shows the calculated TAE growth rate for TFTR and ITER as a function of toroidal mode number n. For TFTR, only a few low-n modes are predicted to be unstable, which is consistent with the experimental observations (Fig. 3). In contrast, in ITER, the most unstable mode shifts to large values of n and there is very little difference between the stability of the various toroidal modes.

Experimentally, only the most unstable modes are observed. Once the stability threshold is exceeded, the first unstable mode begins to grow and eventually saturates nonlinearly, often by "clamping" the fast-ion drive near the point of marginal stability. However, in a burning-plasma experiment, where many modes have essentially the same stability threshold, far more modes will be excited. This effect is already observed to some extent in existing devices. For example, in JT-60U, TAE activity at low field during $\sim$ 350 keV injection is dominated by one or two low n modes [28], while ICRF-tail driven activity at higher toroidal field contains a richer spectrum with $n = 5 - 11$ [29].

To summarize the predictions of the last two sections,

- Fast-ion transport is likely to be less effective.

- The toroidal mode number will shift to higher values.
- The number of unstable toroidal modes will increase.

Taken together, these factors indicate that the relative importance of fast-ion transport and mode overlap in the nonlinear saturation of Alfvén modes is likely to shift in a burning plasma experiment.

E. Energetic Particle Modes

Energetic particle modes are often observed in current experiments. For example, in JT-60U injection of ~ 350 keV neutral beams can drive r-TAE modes [15]. In these experiments, two of the dimensionless parameters that are important in TAE theory, the ratio of the fast-ion velocity to the Alfvén speed v_f/v_A and the normalized fast-particle pressure β_{fast}, are comparable to values predicted in ITER. Nevertheless, these results cannot be directly extrapolated to a burning plasma experiment.

Theoretically, the stability of energetic particle modes is very sensitive to the details of the fast-ion distribution function. This predicted sensitivity is observed experimentally. Figure 7 shows an example of a r-KBM observed in the DIII-D tokamak. In two virtually identically discharges, the r-KBM was strongly unstable when the beam distribution function was peaked at a parallel velocity of $\langle v_\parallel/v\rangle = 0.61$ but was barely observed when the angle of beam injection was slightly altered to $\langle v_\parallel/v\rangle = 0.57$.

In all current experiments where energetic particle modes have been observed, the distribution function is highly anisotropic. Experiments with an isotropic alpha population in the $Q\gtrsim 10$ regime are essential for a thorough understanding of the importance of the various energetic particle modes.

IV. CONCLUSIONS

The birth energy and distribution of alpha particles, their deceleration by

Coulomb scattering, and their spatial transport in the ambient fields of the tokamak are well understood. In the absence of alpha-driven collective instabilities, alpha particles will effectively heat a burning plasma experiment.

The study of fast-ion driven instabilities is a rich and complex field. There are many potentially unstable modes and, for each mode, a whole range of important properties to measure and understand. This complexity has two implications. First, much remains to be learned in current devices. Second, given the complexity of the problem, if a burning plasma experiment is to yield useful information about alpha-driven instabilities, it must have good diagnostics and the experimental capability to vary important parameters such as β_α and the magnetic shear.

There are five issues involving collective instabilities that are unique to a burning plasma experiment.

1. A pure fast-ion distribution function, which requires $Q \gtrsim 10$.

2. Energetic particle modes with an isotropic slowing-down distribution function.

3. Plasma damping at low values of normalized gyroradius ρ^*.

4. Alpha transport with smaller orbits and eigenfunctions.

5. Nonlinear saturation with a sea of unstable modes.

Acknowledgments

My debt to the many experimentalists and theorists who have contributed to the field of fast-ion physics is gratefully acknowledged. This work was partially supported by General Atomics subcontract SC-G903402 under DE-AC03-99ER54463.

Appendix. Justification for the Grades in Table II.

Precessional-drift Fishbone. The frequency was approximately the precession frequency of the beam ions but was about a factor of two smaller than expected [30]. Soft x-ray measurements of the eigenfunction had the expected $n = 1$ structure but were not compared with theory. The polarization in the plasma has never been measured for any fast-ion driven instabiity. With the neglect of a few important terms, the linear stability agreed with theory [31]. The mode-particle pumping theory agreed well with numerous measurements [1]. Nonlinear saturation was successfully explained by a semi-empirical model [27] but a complete theoretical treatment of frequency chirping remains an outstanding problem.

TAE. The measured frequency agrees well with the expected frequency in many devices [32]. The spatial structure is in rough qualitative agreement with theory for some modes in TFTR [33, 34] but agrees rather poorly with theory in DIII-D [35, 36]. There have been several notable successes of linear TAE stability theory, particularly for alpha-driven TAEs in TFTR [34] and comparisons of JET antenna measurements with calculations by the gyrokinetic PENN code [21]. The only attempt to compare theoretical predictions of fast-ion transport with measurements failed [36]. Despite difficulties in explaining the detailed mode structure and fast-ion transport, partial models have successfully predicted some features of nonlinear saturation, including the "predator-prey" model in DIII-D [27], qualitative differences between different regimes in TFTR [37], and "pitch-fork" splitting of the spectral lines in JET [38].

EPM (r-TAE). Quantitative comparisons of the frequency for a few cases have been successful [15, 16]. The eigenfunction has not been measured or realistically calculated. Linear stability is in rough agreement with

experiment [15, 16]. Resonant transport has never been calculated. The nonlinear saturation is probably described by the "predator-prey" model in many cases.

References

[1] W. W. Heidbrink and G. J. Sadler, Nucl. Fusion **34**, 535 (1994).

[2] ITER Physics Expert Group on Energetic Particles, Heating, and Current Drive, et al., Nucl. Fusion **39**, 2471 (1999).

[3] S. J. Zweben, R. V. Budny, D. S. Darrow, S. S. Medley, R. Nazikian, B. C. Stratton, E. J. Synakowski, G. Taylor, and the TFTR group, Nucl. Fusion **40**, 91 (2000).

[4] K.-L. Wong, Plasma Phys. Controlled Fusion **41**, R1 (1999).

[5] J. D. Strachan, S. Batha, M. Beer, et al., Plasma Phys. Controlled Fusion **39**, B103 (1997).

[6] J. P. Gloedbloed, Phys. Fluids **18**, 1258 (1975).

[7] G. J. Kramer, M. Saigusa, T. Ozeki, Y. Kusama, H. Kimura, T. Oikawa, K. Tobita, G. Y. Fu, and C. Z. Cheng, Phys. Rev. Lett. **80**, 2594 (1998).

[8] G. Y. Fu, Phys. Plasmas **2**, 1029 (1995).

[9] A. Fasoli, J. B. Lister, S. Sharapov, et al., Phys. Rev. Lett. **76**, 1067 (1996).

[10] E. D. Fredrickson, N. Gorelenkov, C. Z. Cheng, et al., Phys. Rev. Lett. **87**, 145001 (2001).

[11] R. Nazikian, Z. Chang, E. D. Fredrickson, et al., Phys. Plasmas **3**, 593 (1996).

[12] A. Fasoli, J. B. Lister, S. Sharapov, et al., Nucl. Fusion **35**, 1485 (1995).

[13] L. Chen, Phys. Plasmas **1**, 1519 (1994).

[14] K. McGuire, R. Goldston, M. Bell, et al., Phys. Rev. Lett. **50**, 891 (1983).

[15] N. N. Gorelenkov, S. Bernabei, C. Z. Cheng, et al., Nucl. Fusion **40**, 1311 (2000).

[16] N. N. Gorelenkov and W. W. Heidbrink, Nucl. Fusion **42**, in press (2002).

[17] C. Z. Cheng, N. N. Gorelenkov, and C. T. Hsu, Nucl. Fusion **35**, 1639 (1995).

[18] G. Y. Fu and J. W. van Dam, Phys. Fluids B **1**, 1949 (1989).

[19] M. N. Rosenbluth and P. H. Rutherford, Phys. Rev. Lett. **34**, 1428 (1975).

[20] K. L. Wong, N. Bretz, G. Y. Fu, J. Machuzak, J. R. Wilson, Z. Chang, L. Chen, E. Fredrickson, D. K. Owens, and G. Schilling, Physics Letters A **224**, 99 (1996).

[21] A. Jaun, A. Fasoli, J. Vaclavik, and L. Villard, Nucl. Fusion **39**, 2095 (1999).

[22] W. W. Heidbrink, A. Fasoli, D. Borba, and A. Jaun, Phys. Plasmas **4**, 3663 (1997).

[23] R. R. Mett and S. M. Mahajan, Phys. Fluids B **4**, 2885 (1992).

[24] D. Testa, A. Fasoli, D. Borba, et al., (2001), IAEA TCM presentation.

[25] R. B. White, R. J. Goldston, K. McGuire, et al., Phys. Fluids **26**, 2958 (1983).

[26] H. H. Duong, W. W. Heidbrink, E. J. Strait, T. W. Petrie, R. Lee, R. A. Moyer, and J. G. Watkins, Nucl. Fusion **33**, 749 (1993).

[27] W. W. Heidbrink, H. H. Duong, J. Manson, E. Wilfrid, C. Oberman, and E. J. Strait, Phys. Fluids B **5**, 2176 (1993).

[28] Y. Kusama, G. J. Kramer, H. Kimura, et al., Nucl. Fusion **39**, 1837 (1999).

[29] M. Saigusa, H. Kimura, Y. Kusama, G. J. Kramer, T. Ozeki, S. Moriyama, T. Oikawa, Y. Neyatani, and T. Kondoh, Plasma Phys. Controlled Fusion **40**, 1647 (1998).

[30] D. A. J. Buchenauer, *Fast ion effects on magnetic instabilities in the PDX tokamak*, PhD thesis, Princeton University, 1985.

[31] D. W. Roberts, *Stability studies of PBX-M plasmas with neutral probe beam q-profile diagnostics*, PhD thesis, Princeton University, 1991.

[32] W. W. Heidbrink, Experimental aspects of effects of high-energy particles on alfven modes, in *Theory of Fusion Plasmas (Proc. Joint Varenna-Lausanne Workshop 1994)*, page 49, Bologna, 1994, Editrice Compositori (ISBN 88-7794-066-2), GA-A21811.

[33] R. D. Durst, K. L. Wong, C. Z. Cheng, R. J. Fonck, E. D. Fredrickson, and S. F. Paul, Phys. Fluids B **4**, 3707 (1992).

[34] R. Nazikian, G. Y. Fu, Z. Chang, et al., Phys. Plasmas **5**, 1703 (1998).

[35] W. W. Heidbrink, A. Jaun, and H. A. Holties, Nucl. Fusion **37**, 1411 (1997).

[36] E. M. Carolipio, W. W. Heidbrink, C. Z. Cheng, et al., Phys. Plasmas **8**, 3391 (2001).

[37] K. L. Wong, R. Majeski, M. Petrov, et al., Phys. Plasmas **4**, 393 (1997).

[38] R. F. Heeter, A. F. Fasoli, and S. E. Sharapov, Phys. Rev. Lett. **85**, 3177 (2000).

[39] R. Nazikian, G. Y. Fu, S. H. Batha, et al., Phys. Rev. Lett. **78**, 2976 (1997).

[40] G. Y. Fu and C. Z. Cheng, Phys. Fluids B **4**, 3722 (1992).

[41] A. Fasoli, D. Borba, C. Gormezano, et al., Plasma Phys. Controlled Fusion **39**, B287 (1997).

[42] E. J. Strait, W. W. Heidbrink, A. D. Turnbull, M. S. Chu, and H. H. Duong, Nucl. Fusion **33**, 1849 (1993).

[43] K. L. Wong, R. J. Fonck, S. F. Paul, et al., Phys. Rev. Lett. **66**, 1874 (1991).

[44] W. W. Heidbrink, E. Ruskov, E. M. Carolipio, J. Fang, M. A. van Zeeland, and R. A. James, Phys. Plasmas **6**, 1147 (1999).

[45] S. Bernabei, M. G. Bell, R. Budny, et al., Phys. Plasmas **6**, 1880 (1999).

[46] W. W. Heidbrink, E. Fredrickson, T. K. Mau, C. C. Petty, R. I. Pinsker, M. Porkolab, and B. W. Rice, Nucl. Fusion **39**, 1369 (1999).

[47] J. Candy and M. N. Rosenbluth, Nucl. Fusion **35**, 1069 (1995).

Table I. Relationship between a normal mode of the background plasma and the corresponding energetic particle mode.

Normal Mode	**Energetic Particle Mode**
$n_{fast} \ll n_e$	$\beta_{fast} \sim \beta$
Wave exists w/o fast ions	Fast ions create a new wave branch
Re(ω) unaffected by fast ions	Re(ω) depends on β_{fast}
Fast ions resonate with mode, altering Im(ω)	Fast ions resonate with mode, altering Im(ω)

Table II. "Report Card" on the status of comparisons between theory and experiment for the precessional-drift fishbone, the TAE, and the resonant-TAE instabilities, rated on a traditional A-B-C-D-F grading scale.

Property	**Fishbone**	**TAE**	**EPM**
Frequency	B	A	B
Eigenfunction	C	D	F
Polarization	F	F	F
Linear stability	B	B	C
Resonant transport	A	F	F
Nonlinear saturation	B	C	F

Table III. Comparison of the relative orbit and eigenfunction sizes for DIII-D TAE experiments with anisotropic beam ions, for TFTR TAE experiments with isotropic alphas, and for ITER alpha-driven TAE projections.

Device	Fast ion	ρ/a	Mode width
DIII-D	Beam ions	0.09	$\simeq 0.5a$
TFTR	Alphas	0.05	$\simeq 0.3a$
ITER	Alphas	0.015	$\simeq 0.1a$

Figure Captions

Figure 1. Ratio of the measured slowing down time normalized to the standard Coulomb slowing down time versus the slowing-down time on electrons τ_{se} for sixteen tokamak fast-ion experiments. (Original figure from Ref. [1], with additional TFTR DT alpha point added by Strachan [5].)

Figure 2. Schematic illustration of the approximate frequency, radial location and mode width of observed fast-ion driven normal modes (solid lines) and energetic particle modes (dashed lines) versus poloidal flux for a monotonically increasing q profile. The $n = 3$ shear Alfvén frequency continuum curves (dotted curves) are also shown. From high frequency to low, the acronyms stand for ion cyclotron emission (ICE), compressional Alfvén eigenmode (CAE), triangularity-induced Alfvén eigenmode (NAE), ellipticity-induced Alfvén eigenmode (EAE), kinetic toroidicity-induced Alfvén eigenmode (KTAE), toroidicity-induced Alfvén eigenmode, and kinetic ballooning mode (KBM).

Figure 3. Alpha-particle driven TAEs with toroidal mode numbers $n = 2$-5 in a weak shear DT TFTR plasma. During neutral beam injection the plasma beta is large and the beam ions constitute a significant fraction of the total plasma beta, while the alpha contribution is low. When the neutral beams turn off, the beam ions decelerate more rapidly than the alphas, creating a transient condition where the alpha population dominates the overall fast-ion population (from Ref. [39]).

Figure 4. Theoretical model of "mode-particle pumping" that successfully explained the loss of 45 keV beam ions during fishbone activity in the PDX tokamak. The assumed eigenfunction of the instability as a function of minor radius is fit to the results of a linear MHD calculation of the internal kink mode. A Hamiltonian guiding center code follows the beam orbits in the

assumed MHD electric and magnetic fields. A typical loss orbit is shown. The banana orbit of the beam ion appears to migrate to larger major radius as the ion convectively $\mathbf{E} \times \mathbf{B}$ drifts out of the machine (from Ref. [25]).

Figure 5. (a) Numerical calculation of the linear alpha drive γ/ω versus the product of the poloidal wavenumber k_θ and the alpha gyroradius ρ_α (from Ref. [40]). For small orbit width, the drive term is linearly proportional to the diamagnetic drift of the alpha particles $\omega_{*\alpha}$ (which is proportional to k_θ). When the gyroradius exceeds the poloidal wavelength, the drive decreases. The maximum growth rate occurs when $k_\theta \rho_\alpha \simeq 1$. (b) Toroidal mode number n observed on magnetics versus the toroidal mode that corresponds to $k_\theta \rho_f = 1$ for eight tokamak measurements of fast-ion driven TAEs. The vertical error bar represents the range of toroidal mode numbers that were typically excited. The expected toroidal mode number is approximately $n \simeq aB_T/(qZ_f\sqrt{8E_f m_f})$ for passing particles, where a is the minor radius, B_T is the toroidal field, q is an estimate of the safety factor near $r = a/2$, and Z_f and m_f are the charge and mass of the fast ions. For trapped particles, the maximum drive occurs when n is $\sim 70\%$ smaller [40]. The fast-ion energy E_f is taken as the birth energy for alphas and beam ions and as the energy of an ion out in the tail for ICRF (e.g., 1 MeV for H-minority heating for the JET case in Ref. [41]). Data from Refs. [42, 43, 11, 44, 29, 41, 45, 28, 46].

Figure 6. Normalized TAE growth rate versus toroidal mode number n in TFTR (diamonds) and the International Tokamak Engineering Reactor (ITER) ($\times$). From Ref. [47]. The theory of Ref. [47] neglects the reduction in alpha drive associated with finite orbit width so, in a complete theory, γ/ω in ITER peaks for $n \simeq 25$.

Figure 7. Spectra of magnetic activity for two nearly identical beam-heated DIII-D discharges with negative central shear. For nearly identical

beam power injected, a slight reduction in the average injected pitch angle $\langle v_{\|}/v \rangle$ virtually stabilized the r-KBM activity (from Ref. [44]).

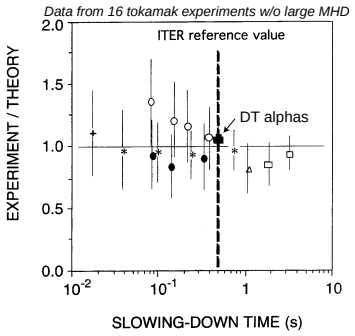

Heidbrink, PoP 25968-DPP, Fig. 1

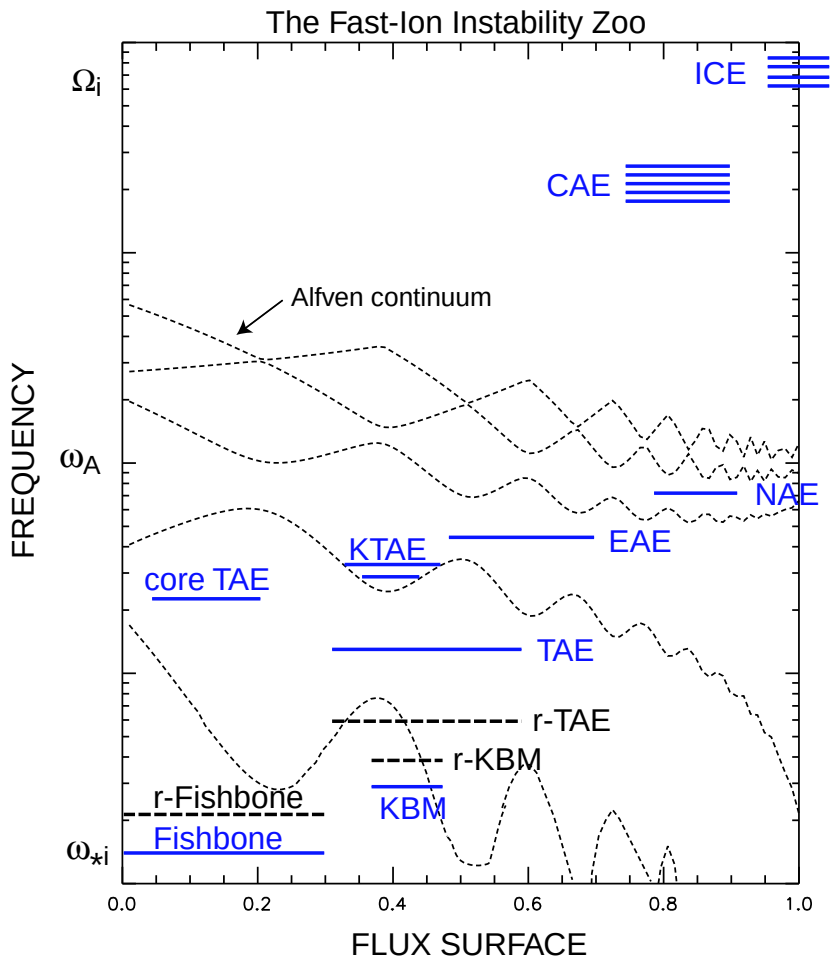

Heidbrink, PoP 25968-DPP, Fig. 2

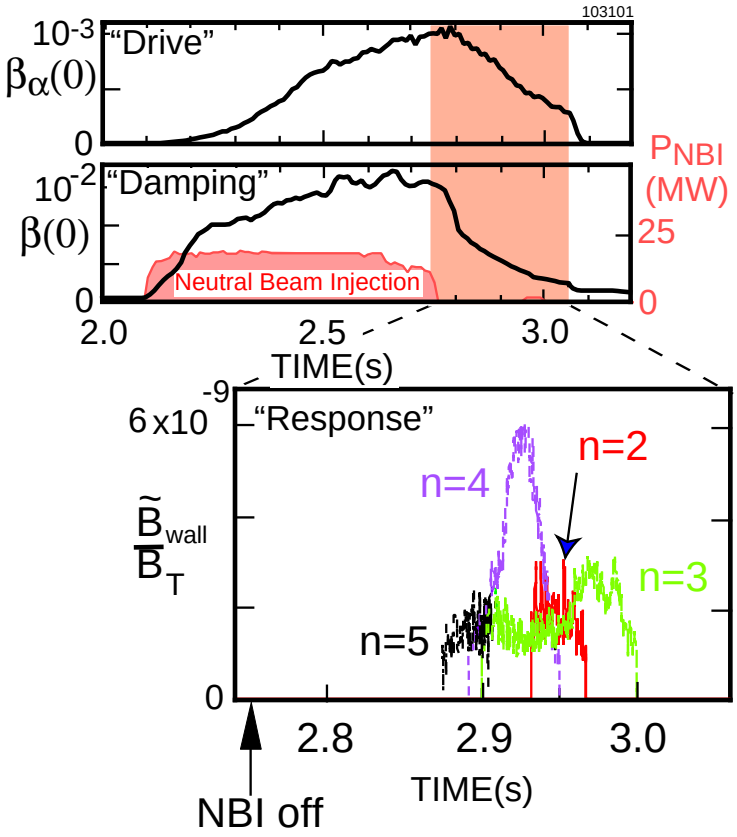

Heidbrink, PoP 25968-DPP, Fig. 3

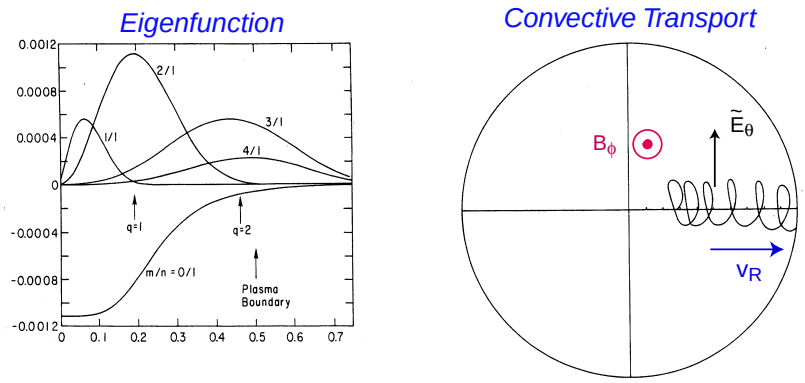

Heidbrink, PoP 25968-DPP, Fig. 4

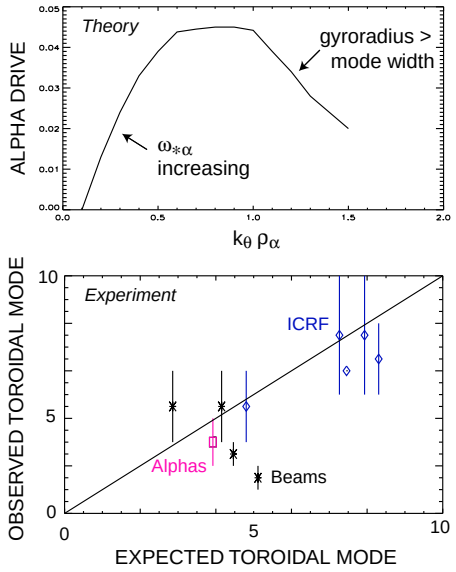

Heidbrink, PoP 25968-DPP, Fig. 5

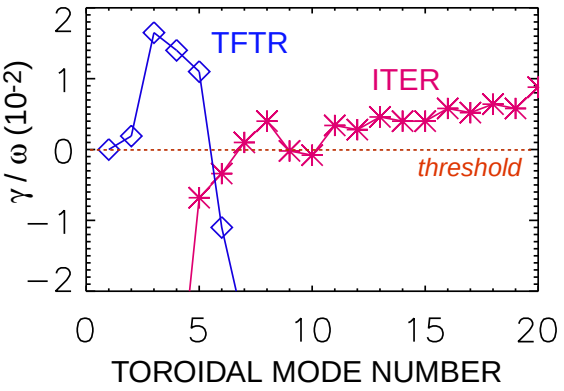

Heidbrink, PoP 25968-DPP, Fig. 6

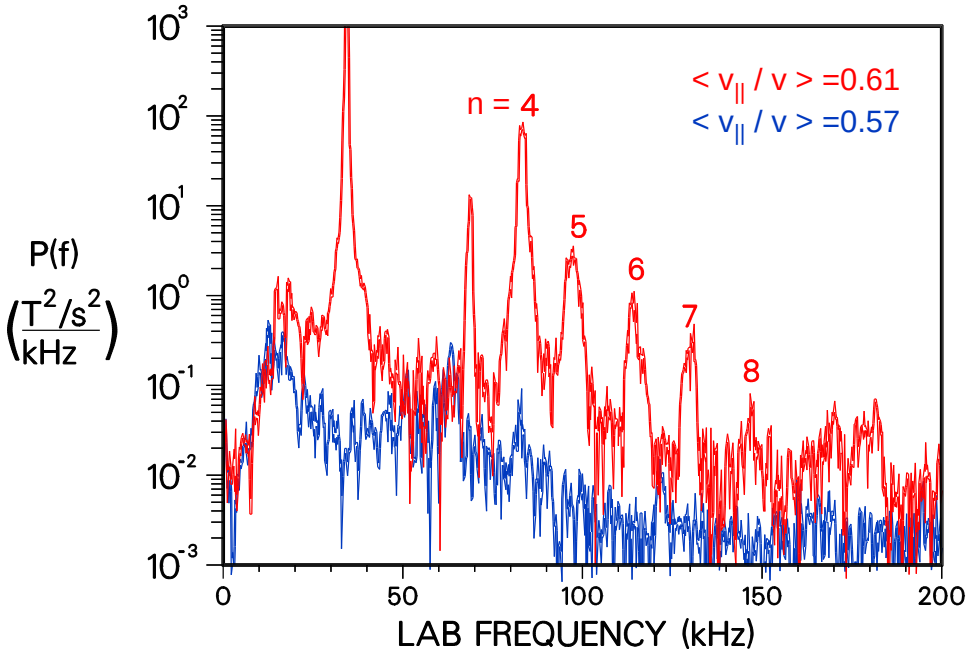

Heidbrink, PoP 25968-DPP, Fig. 7